American Journal of Physics and Applications
2022; 10(2): 38-44
http://www.sciencepublishinggroup.com/j/ajpa
doi: 10.11648/j.ajpa.20221002.13
ISSN: 2330-4286 (Print); ISSN: 2330-4308 (Online)

Dependence of Orbital Feshbach Resonance in ^{173}Yb on Nuclear Hyperfine States

Soumita Mondal[1, 2]

[1]Department of Physics, Shanghai University, Shanghai, China
[2]Department of Physics, Keio University, Yokohama, Japan

Email address:
soumita_phy@keio.jp

To cite this article:
Soumita Mondal. Dependence of Orbital Feshbach Resonance in ^{173}Yb on Nuclear Hyperfine States. *American Journal of Physics and Applications*. Vol. 10, No. 2, 2022, pp. 38-44. doi: 10.11648/j.ajpa.20221002.13

Received: March 9, 2022; **Accepted**: March 24, 2022; **Published**: March 31, 2022

Abstract: Ultracold alkali (^{6}Li, ^{40}K) and alkaline earth atoms (^{87}Sr) have been long sought for the investigation of precision and quantum simulation properties. Feshbach resonance (FR) is an important tool for changing the interaction between atoms by changing the magnetic field strength between the atoms. FR is of two kinds magnetic Feshbach resonance (MFR) and orbital Feshbach resonance (OFR) dealing with one band and two band nature respectively. In OFR the energy difference between open and closed channel is in the range of Fermi energy or even smaller which reduces to zero at no magnetic field. Due to the unique atomic structure of one valence electron in the outermost orbit for alkali atoms they have been used to explore the superfluidity and single-particle phenomena in the same. Due to the atomic structure of alkaline-earth atoms they possess great advantage for quantum simulation and studying quantum many-body matters such as simulating synthetic gauge field, Kondo physics and SU*(N)* physics. In this paper we utilize the opportunity of investigating spin-orbit coupled (SOC) physics in alkaline-earth (AE) atoms like ^{173}Yb atom in two different electronic and nuclear hyperfine states. We discuss the interaction between atoms in the hyperfine states by varying the interatomic distance. Short range potential (between singlet and triplet channel at finite magnetic field) and long-range potential (between open and closed channels at zero magnetic field) will be discussed in detail in this paper. We also discuss the single-particle density-of-states (DOS) in open and closed channel above superfluid phase transition temperature to discuss the normal state properties in two different nuclear hyperfine cases.

Keywords: Ultracold Atoms, Feshbach Resonance, Density-of-States, Ytterbium Atom, Superfluid Phase Transition Temperature

1. Introduction

Since the onset of cold atom experiments quantum simulation in cold atom physics has greatly enriched our understanding of atomic physics and collective oscillation phenomena [1-4]. The study of cold atoms has occupied an important place for the understanding of important Feshbach resonance (FR) phenomena such as magnetic Feshbach resonance (MFR) [5, 6] and orbital Feshbach resonance (OFR) [7-10].

For the investigation of ultracold atoms group 1 atoms such as ^{6}Li and ^{40}K and group 2 alkaline-earth (AE) atoms like ^{87}Sr [11] are trapped under experimentally achievable trap conditions where they are cooled down to the order of micro kelvins. In this stage the interatomic distance (d) becomes inversely proportional to Fermi momentum (k_F). Later experiments were performed in alkaline-earth (AE) like species such as ^{173}Yb to measure interatomic separation in spin singlet (a_+) and spin triplet channel (a_-). Ultracold AE atoms possess unique advantages for the investigation of quantum many-body physics. To understand the detailed role of various nuclear hyperfine states in OFR ^{173}Yb we first consider the understanding of physically important features of AE atoms due to the special electronic structure of AE atoms. The important features of AE atoms are: two-orbital physics, SU*(N)* spin physics, and FR [12].

(i) Two-orbital physics of AE atoms: The outermost *s*-orbital of an AE atom is occupied by two electrons thus for the electronic ground state labelled by $^1S_0$ both the total electron spin and the total angular momentum are zero. For the electronically excited

state labelled by $^3P_0$ one of the two electrons is excited to the p-orbital and the total electronic spin S=1, and because its electronic spin is different from the ground state electronic spin, the dipolar transition between $^3P_0$ and $^1S_0$ is forbidden. As a result, the spontaneous emission is strongly suppressed. Due to this the lifetime of a single atom of a $^3P_0$ state could last up to a few seconds [13]. Considering a mixture of atoms in both the states of $^1S_0$ and $^3P_0$with an orbital degree of freedom that distinguishes them. These two states give rise to a doublet state for the realization of the orbital degree of freedom. The two-orbital physics is important from the viewpoint of precision measurement. The optical transition between these two states is now used for the manufacture of optical clocks with an accuracy of 10^{-19} [13]. Recently the optical coupling has also been found useful for the quantum simulation of spin-orbit coupling (SOC) effect [14]. The advantage of this doublet state is that it can largely avoid the heating problem due to the spontaneous emission. Heating caused by spontaneous emission in optical Feshbach resonance is the main obstacle that prevents the realization of many-body physics when SOC is simulated in degenerate alkali-earth metal atoms.

(ii) SU*(N)* Spin Physics: The fermionic AE atoms also have non-zero nuclear spin, and in particular, the nuclear spin is quite large for many isotopes. For $^1S_0$ and $^3P_0$ states, the angular momentum J=0 with the absence of hyperfine coupling. This leads to the interaction between atoms being independent of nuclear spins. Thus, at zero magnetic field, this system possesses a SU*(N)* symmetry with N=2I+1. For AE atoms and AE-like atoms Bose-Einstein condensate (BEC) state could be achieved at zero magnetic field (strong coupling interaction regime) [15].

These two features discussed previously are unique to AE atoms which have the potential of reopening newest opportunities for various quantum simulation methods. AE atoms have a long history of being utilized for purposes of building optical clocks, and many technologies such as quantum simulation study for performing various previous measurements of many-body physics with AE atoms. We can measure interaction energy with great precision. Due to these reasons ultracold AE atoms have now become a major platform for quantum simulations.

(iii) Feshbach resonace (FR): Another important aspect of ultracold atoms is: controlling of interactions through FR by varying magnetic field. The progress made with AE atoms in the previous two decades has been from the utilization of most important tool of FR. When discussing FR, we come across two important resonance phenomena: MFR [16] and OFR observed in AE [17] and AE like atoms [18-22] respectively. When the interaction energy between atoms could be tuned to be comparable or sometimes larger than the kinetic energy (KE) the conventional perturbation theory fails to capture strong correlation between particles where the physics is not well understood, and the approach of quantum simulation becomes interesting. In order to fully explore the potential of AE atoms in quantum simulation it is highly desirable to develop tools to control interactions between AE atoms. In alkali metal atoms the two most widely used methods for tuning interaction between the interacting atoms are MFR and confinement-induced resonance (CIR). In this regard we focus on two recent developments in AE atoms.

First the electron spin J=0 for both $^1S_0$ and $^3P_0$ states and MFR relies on the electronic spin. It does not exist in $^1S_0$ and $^3P_0$ states of AE atoms. Nevertheless, we use an alternative proposal for developing the concept of orbital degree of freedom to replace the role of electronic spin where nuclear-spin-independent interaction can be tuned by the magnetic field strength. This proposal has been realized by the Munich group and the Florence group and has been used to explore strongly interacting physics in ultracold AE atoms. Secondly CIR also works for AE atoms and could also be utilized to tune the nuclear spin exchanging interaction which can enhance the Kondo effect. This effect has also been observed by the Munich group.

In this perspective we first review the developments of controlling both the spin-independent and spin-dependent-exchanging interactions of AE atoms, respectively, and then we discuss future opportunities for quantum simulation and quantum many-body physics brought by combining these interaction control tools with two-orbital and SU*(N)* physics.

2. Various Kinds of Interaction Between Alkaline-Earth Atoms

In this section we will cover the fermionic nature of AE atomic species in a more detailed and precise manner. The specialty of AE atoms lies in the fact that they have both electronic orbital and nuclear spin degree of freedoms. We denote the two-orbital states $^1S_0$ and $^3P_0$ as $|g\rangle$ and $|e\rangle$ respectively. For simplicity we focus on two out of N nuclear spin states and symbolize them by $|\uparrow\rangle$ and $|\downarrow\rangle$, respectively. The interacting states at short and long interatomic (separation) can be represented by two different kinds of notation. When two atoms are far separated, we consider inter-channel and intra-channel representation which will be taken over in the subsequent section. In the current section we will be discussing the detail of the spin-singlet and spin-triplet channel at short interaction distance.

The general structure of the interaction part can be determined based on the nuclear spin rotational symmetry. Due to this symmetry, we construct bases that are also invariant under the nuclear spin rotation such that the interaction strength could be diagonal in these bases. These bases could be defined by spin singlet and spin triplet channel where the nuclear spin part is either a singlet state or a triplet state that are spin rotational invariant. In this case we only focus on the s-wave interaction where the spatial wave

function is symmetric, the internal state wave function is anti-symmetric. Therefore, the orbital part is a triplet (singlet) state if the nuclear spin part is singlet (triplet). Projection operator $P_{\pm} = |\pm\rangle\langle\pm|$ is brought within the interaction potential as

$$H_{int} = U_{\pm\pm}|\pm\rangle\langle\pm|. \quad (1)$$

Figure 1 below shows interaction potential $(k_F a_s)^{-1}$ vs magnetic field B [G] for $\Delta_m = 1,3$.

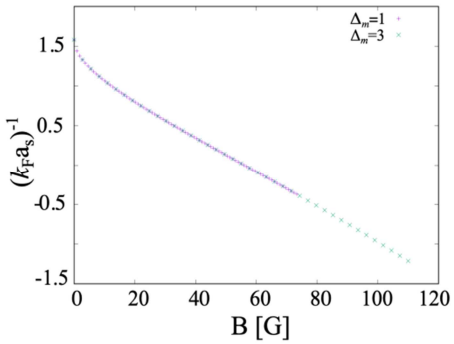

Figure 1. *Scaling in ^{173}Yb gas for Δ_m=1,3.*

2.1. Control of Spin-independent Interaction

The above interaction term represents the coupling of two channels (originating from the diagonal terms at short distance). This interaction can be traced at finite field (limited interaction B>0). This interaction is applied for strongly interacting Fermi gases in topological superfluid. The sum of two interaction potentials acting on $|\pm\rangle$. The interaction between the two channels is tuned by channeling the magnetic field.

Fortunately, ^{173}Yb has a shallow bound state with energy about 4kHz. Hence a FR is accessible in realistic magnetic field strength. Such a resonance is predicted first by theoretical calculation with pseudo-potential model [7] and later has also been confirmed by the multi-channel quantum defect theory [23]. The predicted open-channel scattering has been discussed in. In order to emphasize the important distinction between this resonance and MFR in alkaline-metal atoms we same it as OFR, because here the channel is defined in term of orbital degree of freedom while for FR in alkaline-metal atoms, channels are defined in term of the electronic spin degree of freedom.

The experiments performed by the Florence group and Munich group on ^{173}Yb successfully confirms OFR in ^{173}Yb atom. The general case treated for nuclear spin of ^{173}Yb is 5/2. In this work we consider nuclear states -3/2, -1/2, 1/2, 3/2.

$$|\pm\rangle = \frac{1}{2}[|e,g\rangle_e \pm |g,e\rangle_e][||a,b\rangle_n \mp |b,a\rangle_n]. \quad (2)$$

The interaction potential U_{++} and U_{--} should be independent of the choice of nuclear spin, they should be the same for any combination. Hence the only nuclear spin dependence comes from Δ_m in the expression of δ. If we plot the observables in term of scaled magnetic field strength $B\Delta_m$ the measurement with different nuclear spin combinations should collapse into the same curve. Such a scaling behavior has been observed in aspect ratio measurement by Florence group and thermalization experiment by the Munich group respectively.

Both the experiments referred above found that the lifetime of a degenerate ^{173}Yb Fermi gas nearby OFR can be possibly extended to a few hundred milli-second, sufficiently long to undergo many-body equilibrium. Many-body system nearby a FR is a strongly interacting one with many other interesting features such as BCS-BEC crossover, universal thermodynamics, high transition temperature and pseudo gap physics. Such systems have been extensively studied using MFR in alkali-metal atoms. The difference in many body physics between OFR and MFR in alkaline-metal like atom can be well spotted [18-24].

2.2. Control of Spin-exchange Interaction

This interaction represents the separation of two channels at long distance at zero magnetic field (B=0) (no interaction limit) applied in SU(*N*) and non-equilibrium Kondo physics [25, 26].

3. System in Hamiltonian in ^{173}Yb

In the previous section we discussed the proposals and experiments of the method of controlling both the spin-independent and spin-exchanging interaction in ultracold AE atoms [15, 27-29]. In this section we discuss the applicability of the interaction-controlled physics in ^{173}Yb.

To explain the two-band nature of ^{173}Yb atomic Fermi gas, we consider a model of four component gas. Two electronic spin states and two nuclear hyperfine states. The ground state of a ^{173}Yb atom has two electrons in the outermost s-orbital, forming the spin-singlet state. OFR in a ^{173}Yb Fermi gas uses orbital states ($^1S_0$ and $^3P_0$), as well as two nuclear-spin states with *I=5/2*. Combining these state combinations, we receive open channel and closed channel part as shown below where $||a\rangle$ and $||b\rangle$ represent two of six nuclear-spin states $||I = \frac{5}{2}, I_z = -\frac{5}{2} \sim \frac{5}{2}\rangle$.

Representing the electronic ground and excited states and respectively as $|g\rangle_e$ and $|e\rangle_e$ respectively we simplify the above representation as:

$$\begin{cases}(|o,\uparrow\rangle, (|o,\downarrow\rangle = (|e\rangle_e||a\rangle_n, |g\rangle_e||b\rangle_n),\\ (|c,\uparrow\rangle, (|c,\downarrow\rangle = (|g\rangle_e||a\rangle_n, |e\rangle_e||b\rangle_n),\end{cases}$$

A tunable pairing interaction associated with an orbital feshbach resonance (OFR) is obtained from an inter-band interaction interacting on nuclear-spin triplet ($|-\rangle$) and singlet ($|+\rangle$) as:

$$H_{int} = U_{++}|+\rangle\langle+|+U_{--}|-\rangle\langle-|. \quad (3)$$

Here,

$$|\pm\rangle = \frac{1}{2}[|e,g\rangle_e \pm |g,e\rangle_e][||a,b\rangle_n \mp |b,a\rangle_n], \quad (4)$$

U_{++} and (U_{--}) is an interaction in the nuclear-spin singlet (triplet) channel. In this paper $U_{\pm\pm}$ is treated as constant values.

Considering a model of two-band Fermi gas of 2 electron spin components and 2 nuclear-spin components the combined Hamiltonian can be written as:

$$H = \sum_{\boldsymbol{p},\alpha=o,c,\sigma=\uparrow,\downarrow} \xi_{\boldsymbol{p}}^{\alpha} c_{\alpha,\sigma,\boldsymbol{p}}^{\dagger} c_{\alpha,\sigma,\boldsymbol{p}} +$$
$$+\frac{U_{intra}}{2}\sum_{\boldsymbol{p},\boldsymbol{p'},\boldsymbol{q}} [c_{o,\uparrow,\boldsymbol{p'}+\frac{\boldsymbol{q}}{2}}^{\dagger} c_{o,\downarrow,-\boldsymbol{p'}+\frac{\boldsymbol{q}}{2}}^{\dagger} c_{o,\downarrow-\boldsymbol{p}+\frac{\boldsymbol{q}}{2}} c_{o,\uparrow,\boldsymbol{p}+\frac{\boldsymbol{q}}{2}}+$$
$$c_{c,\uparrow,\boldsymbol{p'}+\frac{\boldsymbol{q}}{2}}^{\dagger} c_{c,\downarrow,-\boldsymbol{p'}+\frac{\boldsymbol{q}}{2}}^{\dagger} c_{c,\downarrow-\boldsymbol{p}+\frac{\boldsymbol{q}}{2}} c_{c,\uparrow,\boldsymbol{p}+\frac{\boldsymbol{q}}{2}}]+$$
$$\frac{U_{inter}}{2}\sum_{\boldsymbol{p},\boldsymbol{p'},\boldsymbol{q}} c_{o,\uparrow,\boldsymbol{p'}+\frac{\boldsymbol{q}}{2}}^{\dagger} c_{o,\downarrow,-\boldsymbol{p'}+\frac{\boldsymbol{q}}{2}}^{\dagger} c_{c,\downarrow-\boldsymbol{p}+\frac{\boldsymbol{q}}{2}} c_{c,\uparrow,\boldsymbol{p}+\frac{\boldsymbol{q}}{2}}$$
$$c_{c,\uparrow,\boldsymbol{p'}+\frac{\boldsymbol{q}}{2}}^{\dagger} c_{c,\downarrow,-\boldsymbol{p'}+\frac{\boldsymbol{q}}{2}}^{\dagger} c_{o,\downarrow-\boldsymbol{p}+\frac{\boldsymbol{q}}{2}} c_{o,\uparrow,\boldsymbol{p}+\frac{\boldsymbol{q}}{2}}]. \quad (5)$$

In the present case of ^{173}Yb we represent open and closed channel by subscript o and c respectively with a band gap of $\frac{\nu}{2} = (2\pi\hbar \times 56\Delta_m)B$ [Hz] originating from the nuclear-spin Zeeman effect and is tunable by adjusting an external magnetic field B (where Δ_m is the difference of the two nuclear-spin states $||a\rangle$ and $||b\rangle$ taken as 3 and 1 respectively). Interaction strength in the open channel in terms of the s-wave scattering length is given by:

$$a_s = a_{intra} + a_{inter}\frac{\sqrt{m\nu}}{1-\sqrt{m\nu}a_{intra}}a_{inter}. \quad (6)$$

Here, $a_{intra} = [a_- + a_-]/2$ and $a_{inter} = [a_- - a_+]/2$ denote the s-wave scattering lengths associated with the intra-channel (U_{intra}) and inter-channel (U_{inter}) interactions when $\frac{\nu}{2} = 0$, respectively, $a_{\pm}$ are the s-wave scattering lengths in the nuclear-spin singlet state ($|+\rangle$) and triplet state ($|-\rangle$), given by:

$$\frac{4\pi a_{\pm}}{m} = \frac{U_{intra} \mp U_{inter}}{1+[U_{intra} \mp U_{inter}]\sum_p^{p_c}\frac{1}{2\varepsilon_{\boldsymbol{p}}}} \quad (7)$$

where p_c is a momentum cutoff The scattering lengths $a_{\pm}$ have recently been measured in a ^{173}Yb Fermi gas as $a_+ = 1900a_0$ and $a_- = 200a_0$, where a_0=0.529 Å is the Bohr radius. We will use these values in our numerical calculations. We also take the typical particle density n=5×10^{13} cm^{-3} observed at the trap center of a ^{173}Yb Fermi gas. We then introduce the Fermi momentum $k_F=[3\pi^2 n]^{1/3}$ for an assumed free Fermi gas with this density. We measure the interaction strength in the open channel in terms of the inverse scattering length, normalized by this Fermi momentum k_F. In this scale, the weak-coupling BCS regime and the strong-coupling BEC regime are characterized as, $(k_F a_s)^{-1} \lesssim -1$ and $(k_F a_s)^{-1} \gtrsim +1$ respectively. The region between the two is called the BCS–BEC crossover region. The equation above indicates the tunability of the scaled interaction $(k_F a_s)^{-1}$ by varying the band gap $\frac{\nu}{2}$ ($\propto$B) by adjusting an external magnetic field B. This is just the OFR-induced tunable pairing interaction. The interaction becomes strongest when $\frac{\nu}{2} = 0$, which gives $(k_F a_s)^{-1}$=1.57. Thus, in this paper we consider interactions at three regions ($(k_F a_s)^{-1} \leq 1.57$) for three specific nuclear-spin states.

We adopt the amended T-matrix approximation (ATMA) for arriving at the single particle spectrum calculation.

Single particle thermal green's function in the α=o, c channel is given by

$$G_{\alpha}(p, i\omega_n) = \frac{1}{i\omega_n - \xi_p^{\alpha} - \sum_{\alpha}(p, i\omega_n)} \quad (8)$$

where, ω_n is the fermion Matsubara frequency. In TMA representation $\sum_{\alpha}(p, i\omega_n)$ is the self-energy correction introduced in the green's function where ω_n is the fermionic Mastubara frequency and $\sum_{\alpha}(p, i\omega_n)$ is the self-energy correction given by,

$$\sum_{\alpha}(p, i\omega_n) = T\sum_{q,\nu_n}\Gamma_{\alpha\alpha}(q, i\nu_n)\, G_{\alpha}^{0}(q-p, i\nu_n - i\omega_n) \quad (9)$$

where ν_n is the boson Matsubara frequency and

$$G_{\alpha}^{0}(p, i\omega_n) = \frac{1}{i\omega_n - \xi_p^{\alpha}} \quad (10)$$

is the bare single particle thermal Green's function in the α channel. The particle number equation is given by

$$N_{\alpha} = 2T\sum_{p,\omega_n} G_{\alpha}(p, i\omega_n) \quad (11)$$

In the normal state above T_c, we only deal with the number equation N, to determine $\mu(T > T_c)$. For numerical calculations, we always assume that $N_{\alpha,\uparrow} = N_{\alpha,\downarrow}$, where $N_{\alpha=o,c,\sigma}$ is the number of Fermi atoms in the $|\alpha,\sigma\rangle$-state. For the interaction parameters we use the value as mentioned previously.

We end this section by discussing the formulation of OFR in ^{173}Yb Fermi atoms.

4. Results

In this section we discuss results at various nuclear spin values m_s= -3/2, -1/2, 1/2, 3/2 for Δ_m= 1,3. We take into consideration the results above superfluid phase transition phenomena T_c. In order to calculate the single-particle excitations in the BCS-BEC crossover region above we calculate single-particle density of states (DOS). In this section we discuss the results for Δ_m= 1,3.

$$\rho_{\alpha}(\omega) = \sum_p A_{\alpha}(p, \omega). \quad (12)$$

Here, the single-particle spectral weight is calculated as $A_{\alpha}(p,\omega) = -\frac{1}{\pi}\,\mathrm{Im}\,[\,G_{\alpha}(p, i\omega_n \to \omega + i\delta)\,]$ where δ is an infinitesimally small positive number. In this paper we carry out analytic continuation by Padé approximation. For the detailed analysis of superfluid phase transition temperature and single-particle spectral weight for Δ_m= 5 has been dealt in detail in our previous publications [18-20]. With the change in nuclear spin values and increasing temperature above T_c we expect some changes in the physical properties of ^{173}Yb gas.

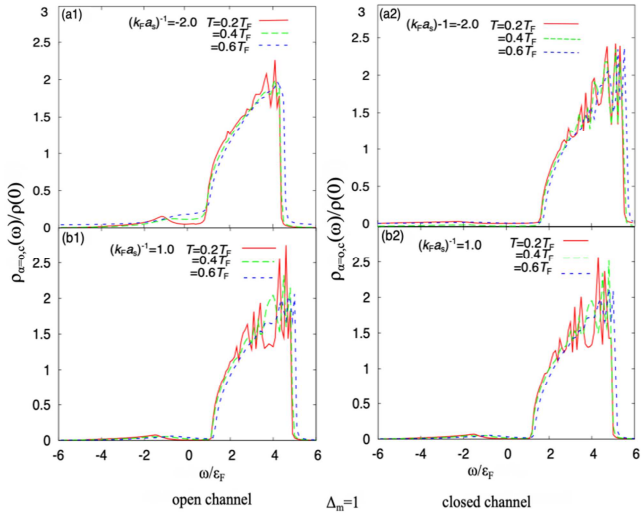

Figure 2. *Representation of single particle density of states in open channel and closed channel particles for Δ_m=1.*

In this section we discuss the single-particle density of states (DOS) above the superfluid critical temperature (T_c) for open and closed channel respectively for Δ_m=1. In figures 2(a1) and (a2) for $(k_Fa_s)^{-1}$=-2.0 in open and closed channel pseudo gap vanishes with increasing temperature and upper peak of closed channel shifts farther away from ω=0. Similarly in figures 2(b1) and (b2) contribution of DOS reduces in ω<0 and the branch for ω>0 shifts away from ω=0 with increasing temperature.

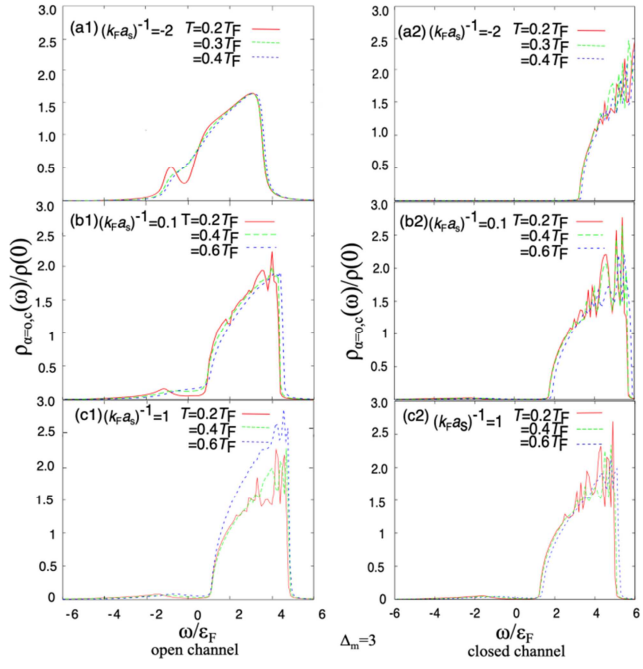

Figure 3. *Representation of single particle density of states in open channel and closed channel particles for Δ_m=3.*

In figure 3 we show DOS in open and closed channel at strength of $(k_Fa_s)^{-1}$= -2.0, 0.1 and 1 respectively at Δ_m= 3 with m_s= -3/2, 3/2. With increasing the interaction strength in the calculation of DOS the gap size increases and decreases in the open channel respectively. The lower peak becomes less prominent, and the dip size decreases. The higher temperature curve shifts away from ω=0 with increasing temperature.

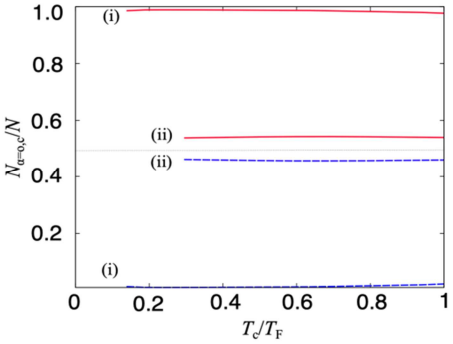

Figure 4. *Representation of number distribution of open channel and closed channel particles for Δ_m=1 at T=0.2T$_F$. Red-solid and blue-dashed curves represent number distribution in open and closed channel respectively at T=0.2 T$_F$. (i) and (ii) stand for interaction strengths -2.0 and 1.0 respectively. The black dotted line represents equal number distribution at $(k_Fa_s)^{-1}$=1.57 (B=0) no interaction strength.*

Figure 4 represents number distribution function for Δ_m=1 in the open ((red) and closed (blue) channel for $(k_Fa_s)^{-1}$=-2.0, 1.0 in curves (i) and (ii) respectively. Number distribution is plotted following equation.
Number equation can be written as:

$$N_\alpha = \int_{-\infty}^{\infty} d\omega f(\omega)\rho_\alpha f(\omega). \quad (13)$$

The large gap structure in $\rho_c(\omega)$ seen in Figure 2 make us expect that the number distribution of atoms in the closed channel almost vanishes in the BCS side.

5. Conclusions

In this paper we explain in detail the dependence of interaction potential on the interatomic distance of the freely attracting ^{173}Yb Fermi atoms. The effect of different nuclear hyperfine states on the physical property of ^{173}Yb Fermi gas has been investigated in detail by the detailed study of single-particle density-of-state (DOS) above superfluid phase transition temperature (T_c). The investigation of normal state properties for different nuclear hyperfine states is important from experimental viewpoint for the future realization of superfluid ^{173}Yb Femi gas in different nuclear hyperfine spin state. Experimental realization of ^{173}Yb rare-earth Fermi gas would be more promising in future which could be highly contributing to the development of cold Fermi gas. Realization of ultracold atomic properties in alkaline-earth (^{87}Sr) or alkaline-earth like (^{173}Yb) elements is important for the detailed realization of Bardeen-Copper-Schrieffer (BCS)-Bose-Einstein-Condensate (BEC) crossover over the periodic table [30-36]. Calculation of superfluid phase transition temperature, single-particle spectral weight and photoemission spectroscopy for Δ_m= 1,3 can be considered as our future work.

Acknowledgements

We thank Inotani, D. for useful discussions. S. M. is

thankful towards Prof. Yongping Zhang Department of Physics Shanghai University China, Keio Leading-edge Laboratory of Science and Technology (KLL) at Keio University and Prof. Priya Mahadevan S. N. Bose National Centre for Basic Sciences (SNBNCBS) for financially supporting this work.

References

[1] Goldman, N., Budich, J. C., & Zoller, P. (2016). Topological quantum matter with ultracold gases in optical lattices. Nat. Phys. 12, 639. doi: https://doi.org/10.1038/nphys3803.

[2] Gross, C., & Bloch, I. (2017). Quantum simulations with ultracold atoms in optical lattices. Science 357, 995. doi: 10.1126/science.aal3837.

[3] Bloch, I., Dalibard, J. & Nascimbène, S. (2012). Quantum simulations with ultracold quantum gases. Nat. Phys. 8, 267. doi: 10.1038/nphys2259.

[4] Bloch, I., Dalibard, J. & Zwerger, W. (2008). Many-body physics with ultracold gases. Rev. Mod. Phys. 80, 885. doi: 10.1103/PhysRevLett.115.135301.

[5] Regal, C. A., Greiner, M., & Jin, D. S. (2004). Lifetime of Molecule-Atom Mixtures near a Feshbach Resonance in ^{40}K. Phys. Rev. Lett. 92, 083201. doi: 10.1103/PhysRevLett.92.083201.

[6] Dieckmann, K., Stan, C. A., Gupta, S., Hadzibabic, Z., C. Schunck, C. H., & Ketterle, W. (2002). Decay of an Ultracold Fermionic Lithium Gas near a Feshbach Resonance. Phys. Rev. Lett. 89, 203201. doi: 10.1103/PhysRevLett.89.203201.

[7] Zhang, R., Cheng, Y., Zhai, H., & Zhang, P. (2015). Orbital Feshbach Resonance in Alkali-Earth Atoms. Phys. Rev. Lett. 115, 135301. doi: 10.1103/PhysRevLett.115.135301.

[8] Pagano, G., Mancini, M., Cappellini, G., Livi, L., Sias, C., Catani, J., Inguscio, M., and Fallani, L. (2015). Strongly Interacting Gas of Two-Electron Fermions at an Orbital Feshbach Resonance. Phys. Rev. Lett. 115, 265301. doi: 10.1103/PhysRevLett.115.265301.

[9] Höfer, M., Riegger, L., Scazza, F., Hofrichter, C., Fernandes, D. R., Parish, M. M., Levinsen, J., Bloch, I., & Fölling, S. (2015). Observation of an Orbital Interaction-Induced Feshbach Resonance in ^{173}Yb. Phys. Rev. Lett. 115, 265302. doi: 10.1103/PhysRevLett.115.265302.

[10] Xu, J., Zhang, R., Cheng, Y., Zhang, P., Qi, R., Zhai, H.(2016). Phys. Rev. A 94, 033609. Reaching a Fermi-superfluid state near an orbital Feshbach resonance. doi: 10.1103/PhysRevA.94.033609.

[11] Zhang, X., Bishof, M., Bromley, S. L., Kraus, C. V., Safronova, M. S., Zoller. P., Rey, A. M. & Ye, J. (2014). Science Vol 345, Issue 6203. doi: 10.1126/science.1254978.

[12] Zhang, R., Cheng, Y., Zhang, P., & Zhai, H. (2019). Controlling the interaction of ultracld alkaline-earth atoms. Nature Reviews Physics, (2020) 2, 213-220. doi: 10.1038/s42254-020-0157-9.

[13] Blagoev, K. B., & Komarovskii, V. A. (1994). Lifetimes of Levels of Neutral and Singly Ionized Lanthanide Atoms. Atomic Data and Nuclear Data Tables, 56, 1. doi: 10.1006/adnd.1994.1001.

[14] Enomoto, K., Kasa, K., Kitagawa, M., & Takahashi, Y. (2008). Optical Feshbach Resonance Using the Intercombination Transition. Phys. Rev. Lett. 101, 203201. doi: 10.1103/PhysRevLett.101.203201.

[15] Gorshkov, A. V., Hermele, M., Gurarie. V., Xu, C., Julienne, P. S., Ye, J., Zoller, P., Demler, E., Lukin, M. D. & Rey, A. M. (2010). Two-orbital SU*(N)* magnetism with ultracold alkaline-earth atoms. Nature Physics volume 6, 289–295. doi: 10.1038/nphys1535.

[16] Bauer, D. M., Lettner, M., Rempe, V. -C., Rempe, G., & Dürr, S. (2009). Control of a magnetic Feshbach resonance with laser light. Nature Physics volume 5, 339–342. doi: 10.1038/nphys1232.

[17] Zhang., Y. -C., Ding, S., & Zhang, S. (2017). Collective modes in a two-band superfluid of ultracold alkaline-earth-metal atoms close to an orbital Feshbach resonance. Phys. Rev. A 95, 041603 (R). 10.1103/PhysRevA.95.041603.

[18] Mondal, S., Inotani, D., & Ohashi, Y. (2017). Closed-channel contribution in the BCS-BEC crossover regime of an ultracold Fermi gas with an orbital Feshbach resonance. J. Phys.: Conf. Ser. 969 012017. doi: 0.1088/1742-6596/969/1/012017.

[19] Mondal, S., Inotani, D., & Ohashi, Y. (2018). Single-particle Excitations and Strong Coupling Effects in the BCS–BEC Crossover Regime of a Rare-Earth Fermi Gas with an Orbital Feshbach Resonance. doi: 10.7566/JPSJ.87.084302.

[20] Mondal, S., Inotani, D., & Ohashi, Y. (2018). Photoemission Spectrum in the BCS–BEC Crossover Regime of a Rare-Earth Fermi Gas with an Orbital Feshbach Resonance. doi: 10.7566/JPSJ.87.094301.

[21] Deng, T. S., Lu, Z.-C., Shi, Y. -R., Chen, J.-G., Zhang, W., & Yi, W. (2018). Repulsive polarons in alkaline-earth-metal-like atoms across an orbital Feshbach resonance. doi: 10.1103/PhysRevA.97.013635.

[22] Kamihori, T., Kagamihara, D., & Ohashi, Y. (2021). Superfluid properties of an ultracold Fermi gas with an orbital Feshbach resonance in the BCS-BEC crossover region. Phys. Rev. A. 103, 053319. doi: 10.1103/PhysRevA.103.053319.

[23] Cheng, Y., Zhang, R., & Zhang, P. (2017). Quantum defect theory for the orbital Feshbach resonance. Phys. Rev. A. 95, 013624 (2017). doi: 10.1103/PhysRevA.95.013624.

[24] Tsuchiya, S., Watanabe, R., & Ohashi, Y. (2009). Single-particle properties and pseudogap effects in the BCS-BEC crossover regime of an ultracold Fermi gas above T_c. Phys. Rev. A 80, 033613. doi: 10.1103/PhysRevA.80.033613.

[25] Zhang, R., Zhang, D., Cheng, Y., Chen, W., Zhang, P., & Zhai, H. (2016). Kondo effect in alkaline-earth-metal atomic gases with confinement-induced resonances. Phys. Rev. A 93, 043601. doi: 10.1103/PhysRevA.93.043601.

[26] Bauer, J., Demler, E., & Salomon, C. (2015). Employing confinement induced resonances to realize Kondo physics with ultracold atoms. Journal of Physics: Conference Series 592 012151. doi: 10.1088/1742-6596/592/1/012151.

[27] Madjarov, I. S., Covey, J. P., Shaw, A. L., Choi, J., Kale, A., Cooper, A., Pichler, H., Schkolnik, V., Williams, J. R., & Endres, M. (2020). High-fidelity entanglement and detection of alkaline-earth Rydberg atoms. Nature Physics volume 16, 857–861. doi: 10.1038/s41567-020-0903-z.

[28] Nakagawa, M., Kawakami, N. (2015). Laser-Induced Kondo Effect in Ultracold Alkaline-Earth Fermions. Phys. Rev. Lett. 115, 135301. doi: 10.1103/PhysRevLett.115.165303.

[29] Ciurylo, R., Tiesienga, E., & Julienne, P. S. (2005). Optical tuning of the scattering length of cold alkaline-earth-metal atoms. Phys. Rev. A 71, 030701 (R) 2005. doi: 10.1103/PhysRevA.71.030701.

[30] Tey, M. K., Stellmer, S., Grimm, R., & Schreck, F. (2010). Double-degenerate Bose-Fermi mixture of strontium. Phys. Rev. A 82, 011608 (R). doi: 10.1103/PhysRevA.82.011608.

[31] Takasu, Y., Honda, K., Komori, K., Kuwamoto, T., Kumakura, Takahashi, M. Y., & Yabuzaki, T. (2004). High-Density Trapping of Cold Ytterbium Atoms by an Optical Dipole Force. Phys. Rev. Lett. 93, 123202. doi: 10.1103/PhysRevLett.93.123202.

[32] Takasu, K., Honda, K., Komori, K., Kuwamoto, T., Kumakura, M., Takahashi, Y., and Yabuzaki, T. (2003). High-Density Trapping of Cold Ytterbium Atoms by an Optical Dipole Force. Phys. Rev. Lett. 90, 023003. doi: 10.1103/PhysRevLett.90.023003.

[33] Fukuhara, T., Takasu, Y., Kumarakura, M. & Takahashi, Y. (2007). Degenerate Fermi Gases of Ytterbium. Phys. Rev. Lett. 98, 030401. doi: 10.1103/PhysRevLett.98.030401.

[34] Fukuhara, T., Sugawa, S., & Takahashi, Y. (2007). Bose-Einstein condensation of an Ytterbium isotope. Phys. Rev. A 76, 051604 (R). doi: 10.1103/PhysRevA.76.051604.

[35] Takasu, Y., & Takahashi, Y. (2009). Quantum Degenerate Gases of Ytterbium Atoms. J. Phys. Soc. Jpn. 78, 012001. doi: 10.1143/JPSJ.78.012001.

[36] Enomoto, K., Takabatake, R., Suzuki, T., Takasu, Y., Takahashi, Y., & Baba, M. (2021). Free-bound excitation and predissociation of ytterbium dimers near the $^1S_0$–$^1P_1$ atomic transition. doi: 10.1103/PhysRevA.104.013118.